Solitonlike states in a one-dimensional nonlinear Schrödinger equation with a deterministic aperiodic potential

Magnus Johansson and Rolf Riklund
Department of Physics and Measurement Technology, University of Linköping, S-581 83 Linköping, Sweden
(Received 26 August 1993)

We study the electronic properties of a one-dimensional deterministic aperiodic nonlinear lattice using a tight-binding form of the nonlinear Schrödinger equation. A nonlinear eigenvalue problem is solved for self-consistent solutions, and the corresponding transmission problem is studied using a two-dimensional nonlinear mapping. When the aperiodicity is chosen according to the Thue-Morse sequence and the nonlinearity is small, we find solitonlike solutions in a similar way as for a periodic lattice. The coupling of an incoming plane wave to these structures results in peaks of perfect transmission in the transmission gaps of the corresponding linear model. Transmission peaks due to dark solitons, and to combinations of several weakly interacting solitons, so called "multisolitons" or "soliton trains" are also found. For larger nonlinearity we find that bounded and diverging solutions are mixed in an intricate pattern; the set of energy values yielding bounded orbits for a given nonlinearity strength showing a Cantor-like structure reminiscent of the linear Thue-Morse system.

I. INTRODUCTION

Motivated by the discovery of incommensurate crystals,[1] quasicrystals,[2] and the experimental fabrication of aperiodic superlattices,[3] extensive theoretical investigations on the electronic and optical properties of deterministic aperiodic materials have been performed. In describing the electronic properties of such materials, special attention has been drawn to a one-dimensional on-site tight-binding model with constant nearest-neighbor hopping. If the hopping integral is normalized to -1, the model is described by the equation

$$V_n\psi_n-\psi_{n+1}-\psi_{n-1}=E\psi_n\ , \tag{1}$$

where the sequence of on-site potentials V_n is deterministic and aperiodic. This equation is equivalent to a discretized time-independent one-dimensional Schrödinger equation with a deterministic aperiodic potential.

The investigations have shown that the properties of the spectrum of allowed energies E and the corresponding electronic wave functions ψ_n depend critically on the choice of aperiodicity in the on-site potential. For incommensurately modulated systems, where the on-site potential takes a continuous set of values, the generic[4] property seems to be that for small modulations the energy spectrum is absolutely continuous and the corresponding wave functions extended, while for large modulations the spectrum has a pure point character with exponentially localized eigenstates. For intermediate modulations, one either finds mobility edges separating extended and localized states, or one finds a sharp energy-independent metal-insulator transition at some particular modulation amplitude, where the spectrum is singular continuous and the wave functions are "critical" (non-normalizable but not extended in the usual fashion).

In models for one-dimensional quasicrystals or aperiodic superlattices the on-site potential is restricted to take values from a finite set of numbers. In the most studied cases, the on-site potential is given by a binary sequence generated by some substitution rule. Some prototype sequences showing qualitatively different electronic properties are the Fibonacci, Thue-Morse,[5] and Rudin-Shapiro[6] sequences. The Fibonacci model, which was the earliest studied of those,[7] has been shown to have a singular-continuous energy spectrum consisting of a Cantor set of zero Lebesgue measure.[8] The corresponding wave functions are all critical.[9] In the Thue-Morse model, extended, "Bloch-like," wave functions have been shown to exist,[10] just like in a periodic system, but the energy spectrum is singular continuous also for this case.[11] Finally, the Rudin-Shapiro sequence displays mainly localized states,[12] and the energy spectrum is proposed[13] to have a pure point character for generic values of the modulation strength. In this context, one should notice that sufficient conditions for model (1) with a substitutionally generated on-site potential to have a singular-continuous energy spectrum have been derived,[14] but those conditions are not fulfilled either for the Thue-Morse or the Rudin-Shapiro cases.

The tight-binding Eq. (1) is a very simple electronic model for (quasi-)one-dimensional systems, where both electron-electron and electron-lattice interactions are neglected. One might therefore ask whether the above discussed features of the different aperiodic systems will be observable in a real physical material, where such interactions inevitably are present. A step in this direction was taken by adding a Hubbard-type on-site electron-electron interaction to the Hamiltonian in (1), treated within the mean-field approximation.[15] It was shown that including the interaction term would for the incommensurate Harper-Aubry model destroy the singular-continuous character of the spectrum, while for the Fibonacci model it would be intact. The effect of introducing this type of interaction in other aperiodic systems, as well as the effect of going beyond the mean-field approxi-

mation, is still an open question.

In this paper we will study the influence of adding other types of interaction to the ordinary tight-binding Eq. (1), leading to the discrete nonlinear Schrödinger equation,

$$V_n\psi_n-\psi_{n+1}-\psi_{n-1}+\alpha|\psi_n|^2\psi_n=E\psi_n \ , \tag{2}$$

where α gives the strength of the nonlinear interaction. This equation appears in a number of different applications in solid-state physics, the Holstein model for large polarons in a molecular-crystal chain being perhaps the most famous example.[16] In this model, the nonlinear term describes the static short-range electron-phonon interaction, the parameter α being given by

$$\alpha=-\frac{A^2}{M\omega_0^2} \ , \tag{3}$$

where A is the electron-lattice coupling constant, M is the molecular mass, and ω_0 the Einstein frequency.[16] The same model, but with opposite sign for α, applies when studying holes instead of electrons. As examples of other applications where Eq. (2) appears, we mention the treatment of the nonlinear optical response of dielectric or magnetic superlattices.[17] The discussions in this paper will, however, mainly be concerned with general properties of Eq. (2) rather than any specific physical model. Thus, even if our starting point is the electronic tight-binding model, the same discussion will apply for example to the optical model, provided that ψ_n is interpreted as an electromagnetic-field amplitude rather than an electronic-wave-function coefficient.

If the wave function has a slowly varying envelope, one can replace the differences in (2) with derivatives and obtain the continuous nonlinear Schrödinger equation. (In the Holstein model, this is the condition that characterizes a large polaron.) For periodic systems, with $V_n\equiv 0$, it is then easy to show that, in addition to the usual Bloch states well known from linear theory, a localized wave function of the form

$$\psi_n=\frac{C}{\cosh[\gamma(n-n_0)]} \ , \tag{4}$$

with $\gamma=|C|\sqrt{|\alpha|/2}$, will also be an exact solution with energy $E=-2-\gamma^2$ to the continuous equation when α is negative. C and n_0 are arbitrary constants determining the amplitude and center of the wave function, respectively. When properly normalized, this solution describes the large polaron constituting the ground state of the Holstein model in the range where the continuum approximation is valid.[16] Apart from a space- and time-dependent phase factor, this will also be a solution to the time-dependent nonlinear continuous Schrödinger equation, describing an envelope soliton propagating distortionless with velocity v through the lattice;[18] the center being given by $n_0=vt$. If α is positive, one instead finds for $E=-2+2\gamma^2$ a solution of the form

$$\psi_n=C\tanh[\gamma(n-n_0)] \ , \tag{5}$$

with $\gamma=|C|\sqrt{|\alpha|/2}$, which in the time-dependent case describes a so called dark soliton[18] appearing as a propagating dip in a constant background intensity.

In the case where V_n are random numbers, Eq. (2) describes nonlinear wave propagation in disordered systems, which has been an intensively studied subject in recent years.[19] The question whether the exponential Anderson localization[20] in linear disordered systems will be destroyed by a nonlinear interaction has turned out not to have a unique answer,[21] since one can pose problems where Anderson localization is either intact (or slightly enhanced)[22] or weakened.[23] This ambiguity origins in the facts that for a nonlinear system (i) the propagation of a pulse is not equivalent to the propagation of a single-frequency wave, and (ii) transmission problems where the input or output amplitudes, respectively, are held constant are nonequivalent.

The subject of deterministic aperiodic systems with nonlinear properties has so far been much less studied than the periodic or random nonlinear systems. Most of these studies concern optical transmission properties of superlattices consisting of nonlinear materials arranged in a Fibonacci sequence.[24,25] In Ref. 24, using a nonlinear transfer-matrix technique relying on a slowly varying envelope approximation, solitonlike structures yielding perfect transmission were found when the linear optical path in each slab was chosen as $n\pi$, where n is an integer. However, for this parameter value the linear transmission is also perfect, since the incident light will not be affected by the quasiperiodicity.[26] More exactly, the polynomial invariant of the trace map[7] of the linear model is zero,[26] which for the tight-binding model (1) would correspond to choosing all V_n equal. In Ref. 25, where a model more similar to our Eq. (2) was used, no evidence of solitons was found, and the field envelopes were found to be irregular and fast oscillating.

Recently, studies of electron-lattice-coupled systems where the electronic part of the Hamiltonian is described by either the Harper-Aubry model[27] or the Fibonacci model[28] have been reported. In Ref. 27, the time evolution of an initial electronic state is numerically simulated as it interacts with a harmonic lattice via a symmetrized deformation potential, and it was shown that for the subcritical region of the Harper-Aubry model (i.e., the region where all eigenstates are extended) localized polarons are created. For the Fibonacci system, localization due to lattice relaxation was found in Ref. 28, where a modified Su-Schrieffer-Heeger (SSH) model was used. Although the models studied in those papers are quite different from the model investigated here, we will see that the nonlinearity term in Eq. (2) will cause localization in a similar way.

We will in the rest of this paper mainly focus our investigations on the case where the V_n in Eq. (2) are chosen according to the (nonquasiperiodic) Thue-Morse sequence. The reason for this is that the existence of extended, Bloch-like states in the linear model suggests the possibility of developing solitonlike structures in a similar way as for periodic systems when a small nonlinearity is added. We will in Sec. II show the existence of such structures when Eq. (2) is solved for a finite chain using fixed boundary conditions and a self-consistent iteration procedure. In Sec. III we investigate the corresponding

stationary transmission problem with a fixed output, and show that the coupling of the incident plane wave to such "bright" solitons leads to transmission resonances in the transmission gap of the corresponding linear system. Transmission resonances corresponding to "dark" solitons are also found. Finally, in Sec. IV we study the transmission problem for the case when the nonlinearity is comparable in strength to the on-site potential and hopping integral, and show that bounded and diverging solutions are mixed in an intricate pattern in the (E,α) plane.

II. THE SELF-CONSISTENT PROBLEM

In this section, we will study solutions of Eq. (2) for a finite system of length N with fixed boundary conditions, i.e., $\psi_0=\psi_{N+1}=0$. The normalized solution of the corresponding linear problem ($\alpha=0$), obtained by direct matrix diagonalization, is taken as a starting point for an iteration procedure which is repeated until self-consistency is obtained. In each step, the wave function is normalized, i.e., $\sum_{n=1}^{N}|\psi_n|^2=1$. For comparison, we first make a short discussion of the periodic case ($V_n\equiv 0$) before we turn our attention to the aperiodic Thue-Morse and Fibonacci chains.

For the periodic system, the lowest-energy state will for negative, intermediate values of α ($\alpha_{\min}<|\alpha|<\alpha_{\max}$) to a very good approximation be given by the soliton (polaron) solution (4), where normalization gives

$$|C|=\sqrt{\gamma/2}=\sqrt{|\alpha|/8};\quad \gamma=|\alpha|/4\ . \tag{6}$$

When $|\alpha|<\alpha_{\min}$, $\alpha_{\min}$ depending on N, the width of the soliton becomes too large to make it compatible with the fixed boundary conditions, while for $|\alpha|>\alpha_{\max}$ it becomes so narrow that the discreteness of the lattice becomes important. For α positive, one finds a similar solution for the highest-energy state instead, with the difference that the wave function changes sign at each site. We show in Fig. 1 the state obtained for a chain length of 1024 sites when $\alpha=0.1$. The absolute value of the wave-function coefficients is very well fitted by Eq. (4) with C and γ given by (6).

In studying the Thue-Morse system, we let the on-site potential V_n be generated by the binary substitution rule

$$A\rightarrow AB,\quad B\rightarrow BA\ . \tag{7}$$

By applying this rule to a seed A and iterating it j times, one obtains the jth generation of the Thue-Morse sequence consisting of 2^j letters. This means that the first few generations of the sequence are given by A, AB, $ABBA$, $ABBABAAB$, $ABBABAABBAABABBA$, ... The infinite sequence is then defined as the fixed point of the rule (7), and a physical structure can be obtained by distributing two kinds of atoms along a chain like the A's and the B's in the sequence. To obtain the on-site potential V_n, one associates a value $V_n=+V$ for every site occupied by an A atom, and a value $V_n=-V$ for every site occupied by a B atom. Since the qualitative behavior of the Thue-Morse system is independent of the strength of the on-site potential,[10] we will hereafter, if nothing else is stated, use the specific value $V=1$ in our numerical calculations. For the infinite linear system described by (1), a countable dense set of energy values in the spectrum exists, such that the corresponding eigenstates are extended.[10] Those are all doubly degenerate, except for those located at

$$E=\pm\sqrt{V^2+1}\pm 1\ , \tag{8}$$

giving the lowest- and highest-energy states and the states at the boundaries of the central gap, respectively. Since having the Fermi energy located at those states correspond to the cases of an empty, filled, and half-filled band, respectively, their nature should be most important for the conduction properties of the system.

For a finite system, the energies (8) will be in the spectrum for every generation $j\geq 3$ if periodic boundary conditions ($\psi_{N+1}=\psi_1$, $\psi_0=\psi_N$) are used. The eigenstates will be similar in that their modulus will take only three

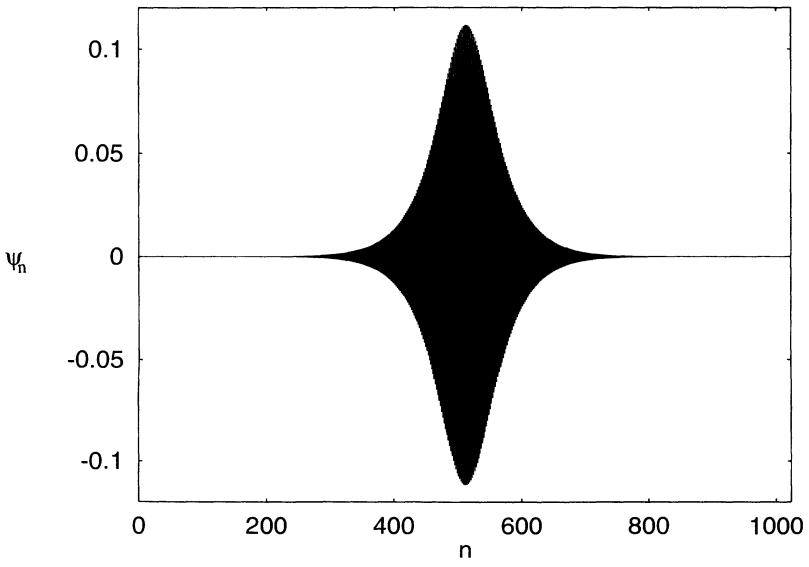

FIG. 1. Normalized wave function corresponding to the highest energy obtained as a self-consistent solution to (2) when $V_n\equiv 0$, $\alpha=0.1$, and $N=1024$. The energy E is given by $E=2.000\,625\,076\ldots\approx 2+\gamma^2=2+\alpha^2/16$.

different values[10] [$|\psi_0|$ and $(\sqrt{V^2+1}\pm V)|\psi_0|$], repeated in a different way and with different signs for the four different energies. Using fixed boundary conditions, the energies (8) will no longer give exact solutions to (1), but for large systems they will be a very good approximation. We show in Fig. 2(a) the state with highest energy $E=2.4142108\ldots\approx\sqrt{2}+1$ for a chain containing 1024 sites ($j=10$). Each of the three subsequences of wave amplitudes shows a sinusoidal modulation just as for a periodic system.

When the nonlinearity constant α is increased from zero, we find that the highest-energy state, just as for the periodic case, develops into a solitonlike structure localized around the center of the chain. Figure 2(b) shows the case when $\alpha=0.01$. The sequence of highest amplitudes are nicely fitted by Eq. (4) with $C\approx0.167$ and $\gamma\approx0.019$. The other two amplitude sequences also follow (4) with the same γ but with the values of C divided by $\sqrt{2}+1$ and $(\sqrt{2}+1)^2$, respectively. One should notice that the value of γ is larger than the value given by (6) by roughly a factor of 7.6, i.e., for a given strength of the nonlinearity the Thue-Morse chain will produce a more localized state than the periodic chain will. A similar behavior is seen for the state just below the central gap, i.e., with $E\approx-\sqrt{2}+1$. The localization of this state will, however, be weaker than for the highest-energy state, the value of γ differing only by a factor of approximately 1.4 from the one given by (6). For negative α, the lowest-energy state and the state just above the central gap will show the same type of behavior, the values of γ and C being roughly equal to the values obtained for the highest-energy state and the state just below the central gap, respectively, when α takes the corresponding positive value.

The development of such solitonlike structures, almost exactly fitted by Eq. (4), in the Thue-Morse chain is a

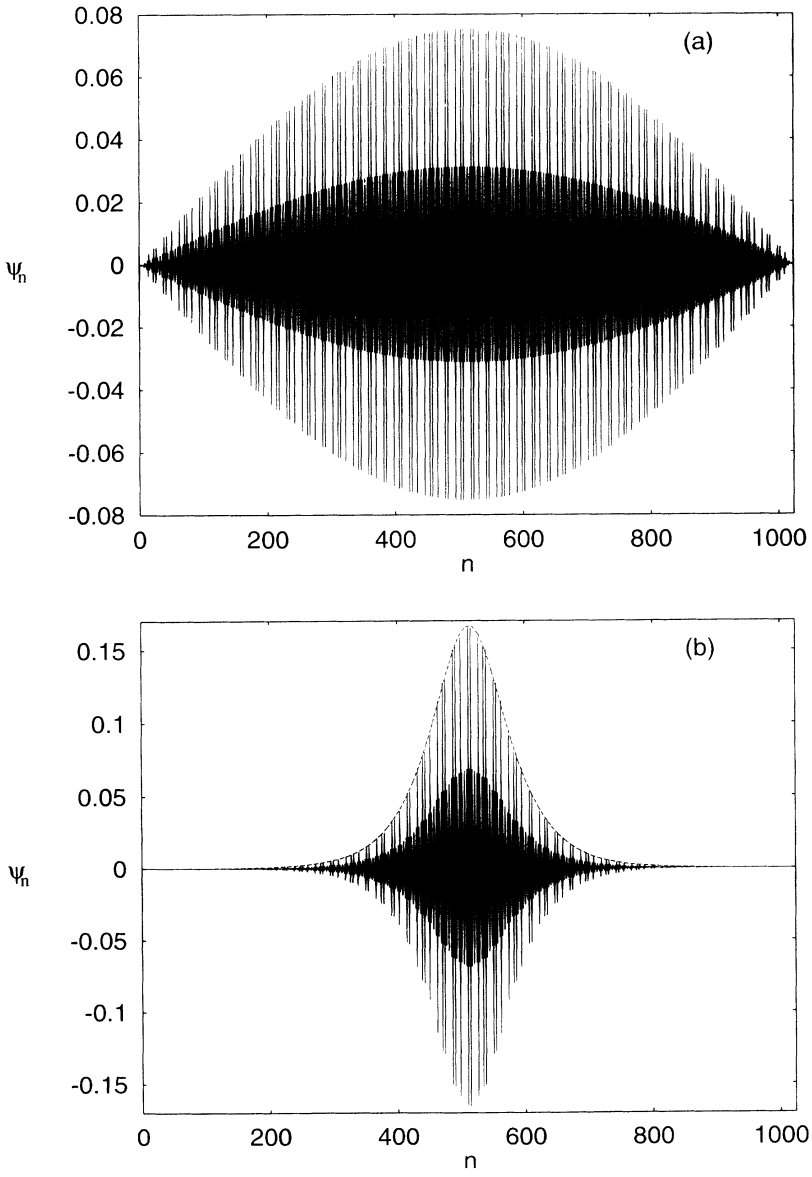

FIG. 2. (a) Highest-energy state for the linear Thue-Morse chain using fixed boundary conditions when $N=1024$. The energy is $E=2.4142108\ldots$. (b) The self-consistent wave function obtained when $\alpha=0.01$ using the state in (a) as initial condition. The energy is $E=2.4143202\ldots$. The dashed line is a plot of the function $0.167/\cosh[0.019(n-513)]$.

striking example showing the similarity of the properties of this aperiodic chain to those of a periodic one. We will in the next section show that these structures give rise to peaks of perfect transmission in linear gap regions of the corresponding transmission spectrum, just as for a periodic system. However, the bulk localization caused by the nonlinearity term in (2) is a phenomenon which is present also for other systems. To give an example of this we have also studied the Fibonacci model, where the on-site potential is obtained in the same way as for the Thue-Morse model, but using the substitution rule

$$A \rightarrow AB, \quad B \rightarrow A \tag{9}$$

instead of (7). In Fig. 3(a) we show the highest-energy state for the linear Fibonacci model ($\alpha=0$); a critical state which is self-similar and neither localized nor extended in the usual fashion. With $\alpha=0.01$, we obtain as the self-consistent solution the state shown in Fig. 3(b). Comparing Figs. 2(b) and 3(b), we see that although the Fibonacci state possesses no smooth, solitonlike envelope, the length of the region where it will be localized is approximately the same as for the Thue-Morse model with the same value of α. In the transmission problem, we find that coupling of a plane wave to the type of nonlinear Fibonacci states discussed here will yield a nonzero, but not perfect, transmission. The state in Fig. 3(b) has a similar structure as the states localized by lattice relaxations obtained in Ref. 28 using a SSH model, indicating that the nonlinearity-induced localization of this kind of states is qualitatively independent of the particular model chosen.

One should also note that, although the qualitative behavior of the Thue-Morse system is independent of the modulation strength V, quantitative properties are in general not. In our study, we find that a larger value of V makes the system more sensitive to the nonlinear pertur-

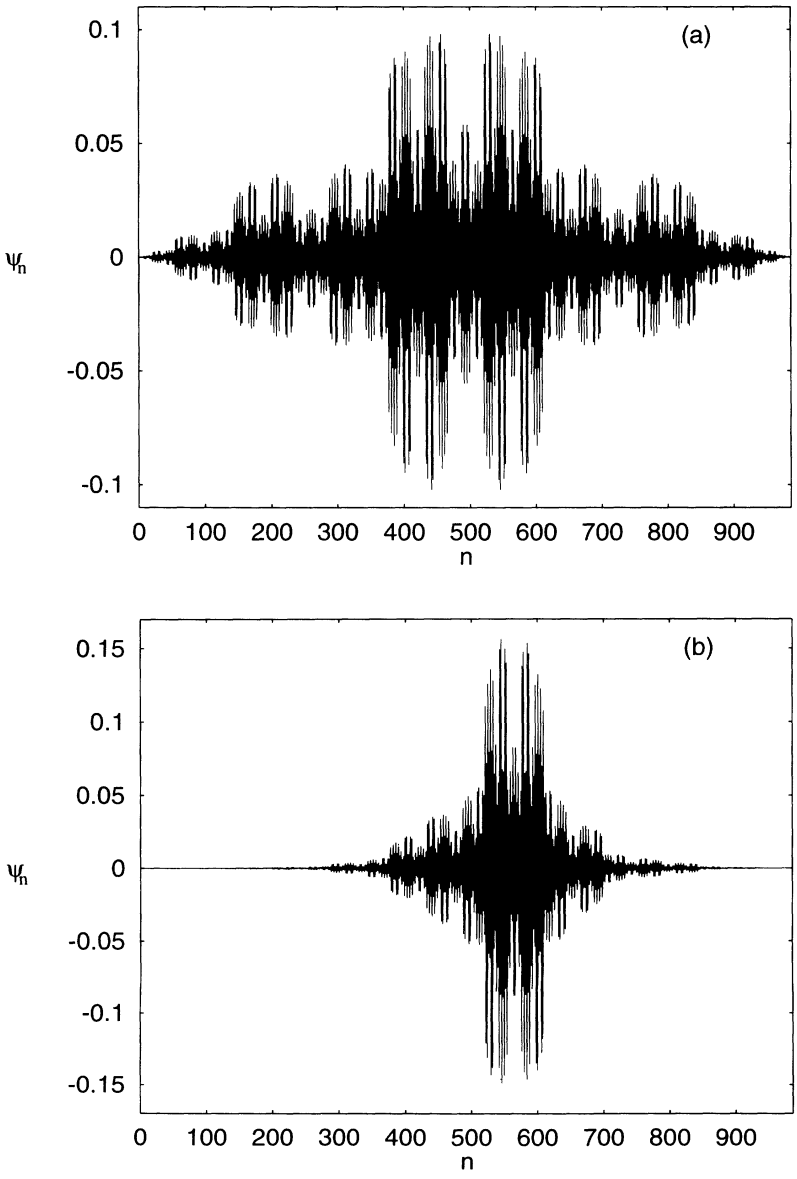

FIG. 3. Same as Fig. 2 but for the Fibonacci model instead of the Thue-Morse model. The chain length is $N=987$ and the energies are in (a) $E=2.507\,702\,8\ldots$ and in (b) $E=2.507\,809\,5\ldots$.

bation. For example, when $V=10$ it only takes a value of α of the order of 5×10^{-6} for the highest-energy state to obtain the same value of γ as in Fig. 2(b).

III. THE TRANSMISSION PROBLEM, SMALL NONLINEARITY

The system that will be considered in this section consists of a finite, nonlinear, aperiodic chain described by Eq. (2) embedded in a infinite, linear, periodic chain described by Eq. (1) with $V_n\equiv0$. We will study the problem of stationary transmission through this nonlinear chain; the wave functions in the linear parts taken as single Bloch waves specified by a wave vector k. We thus have the following problem:

$$\psi_n=R_0e^{ikn}+R_1e^{-ikn},\quad n\le1\ ,$$
$$(V_n+\alpha|\psi_n|^2)\psi_n-\psi_{n+1}-\psi_{n-1}=E\psi_n,\quad 1\le n\le N\ , \tag{10}$$
$$\psi_n=Te^{ikn},\quad n\ge N\ ,$$

where R_0, R_1, and T define the incoming, reflected, and outgoing wave amplitudes, respectively. The transmission coefficient t is defined in the usual way as

$$t=\frac{|T|^2}{|R_0|^2}\ . \tag{11}$$

For this kind of nonlinear problem, it is in general not possible to define uniquely the transmission coefficient as a function of incident intensity, since for a given value of R_0 there may be several combinations of (R_1,T) satisfying (10), leading to the phenomenon of multistability.[29] Instead we will consider the case where the outgoing amplitude T is fixed, which as we will see uniquely determines $|R_0|$ and $|R_1|$ and thereby the transmission coefficient t.

Since ψ is a complex quantity, Eq. (2) will give rise to a real four-dimensional nonlinear mapping. However, because of current conservation $[J\equiv\mathrm{Im}(\psi_n\psi^*_{n-1})=|T|^2\sin k]$, it can be reduced to a two-dimensional one[30] using the quantities

$$x_n=\frac{|\psi_n|^2}{|T|^2},\quad y_n=\frac{\mathrm{Re}(\psi_n\psi^*_{n-1})}{|T|^2}\ . \tag{12}$$

The reduced mapping will then take the form

$$x_{n-1}=\frac{1}{x_n}(y_n^2+\sin^2k),\quad \forall n\ ,$$
$$y_{n-1}=-y_n+x_{n-1}(V_{n-1}+\alpha|T|^2x_{n-1}-E)\ , \tag{13}$$
$$1\le n\le N+1$$

with initial conditions $x_N=1$, $y_{N+1}=\cos k$. By iterating (13) from the output end to the input end of the nonlinear chain and using (10) and (12) to express x_0, x_1, and y_1 in R_0, R_1, T, and k, we can solve for $|R_0|$ and by (11) obtain the transmission coefficient as

$$t=\frac{4\sin^2k}{x_1+x_0-2y_1\cos k+2\sin^2k}\ . \tag{14}$$

For the linear, periodic chain the energy E is related to the Bloch vector k through $E=-2\cos k$. However, when investigating the system defined by (10) we will for the sake of generality assume, as in Ref. 30, that E and k can be varied independently. This will in reality be the case, when interface regions of space charge giving rise to a shift in the relative energy scales of the linear and nonlinear parts of the chain are considered. Of course, our model is too simple to take such effects into full account, but as long as the nonlinear part of the chain is large enough so that the extent of the interface regions can be neglected, the main qualitative effect of including such regions should be a simple shift in the energy scales. (See the first paper of Ref. 30 for a further discussion about the justification of this assumption.)

Since we here primarily are interested in investigating the effect of the solitonlike wave functions found in Sec. II for the nonlinear Thue-Morse system on the transmission spectrum, we will concentrate our studies to regions close to the energy values given by (8). We will show here results obtained around the energy $E=\sqrt{2}-1$, i.e., just above the central gap of the linear model, remembering that the qualitative behavior will be the same for $E=-\sqrt{2}-1$, and also for $E=\pm\sqrt{2}+1$ if α is changed to $-\alpha$ and k to $\pi-k$. The value of k will be chosen to be a small value, since we are studying the region around a lower band edge. However, if k is too small, the transmission peaks will be too narrow to be visible in our plots. We will therefore mainly use a value of $k=0.01$ in the results presented in this section. In Fig. 4(a) we show how the transmission coefficient varies with energy for a linear Thue-Morse chain with $N=1024$ sites in a small energy interval around the upper edge of the central gap. The leftmost peak will, as $k\to0$, be located at $E=\sqrt{2}-1$ and correspond to the case where x_n (or equivalently $|\psi_n|^2$) takes only three different values, as discussed in Sec. II. Since the current density is given by $J=|T|^2\sin k$, this is the limiting case when no current flows through the system. For $k=0.01$, there will be a small shift of the peak energy ($E\approx0.414\,228\,2$) and small fluctuations in the field intensity. For larger values of E, the field intensities x_n will be periodically modulated, and transmission peaks will result as soon as the length of the Thue-Morse chain is equal to an integer times the wavelength of the modulation of the field intensity.

In studying the case with a small, but nonzero, nonlinearity in the system, we see from (13) that the nonlinearity enters only through the product $\alpha|T|^2$ in the map. Consequently, varying the nonlinearity constant is equivalent to varying the transmitted intensity, and we may therefore fix one of them and only use the other as a variable. We choose to work at a fixed transmitted intensity $|T|^2=1$ and study the behavior for various α. In Fig. 4(b) we show the transmission coefficient as a function of energy in the same energy region as in Fig. 4(a) for the case when $\alpha=-10^{-8}$. In the linear transmitting region, we get the same transmission peaks as in (a), although shifted a small amount in the negative direction. In the linear gap region, however, new peaks will appear, some of them showing perfect transmission with $t=1$. The distribution of the field intensity corresponding to some of these peaks is shown in Fig. 5. In Figs. 5(a) and 5(b)

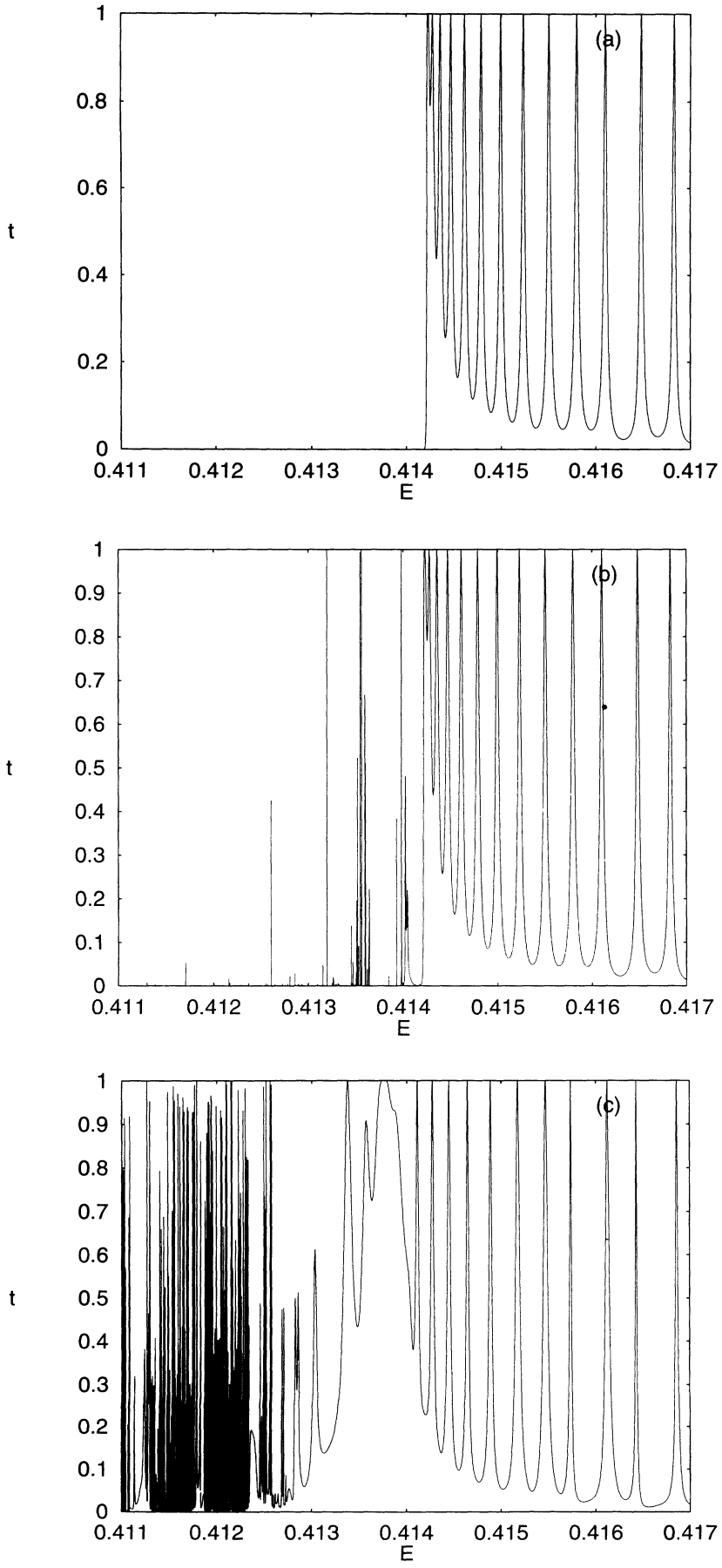

FIG. 4. Transmission coefficient t versus energy E for a Thue-Morse chain with 1024 sites in a region around the energy $E=\sqrt{2}-1$ for (a) a linear chain ($\alpha=0$) and (b),(c) weakly nonlinear chains with $\alpha=-10^{-8}$ and $\alpha=-10^{-4}$, respectively. In all figures, $k=0.01$ independent of E.

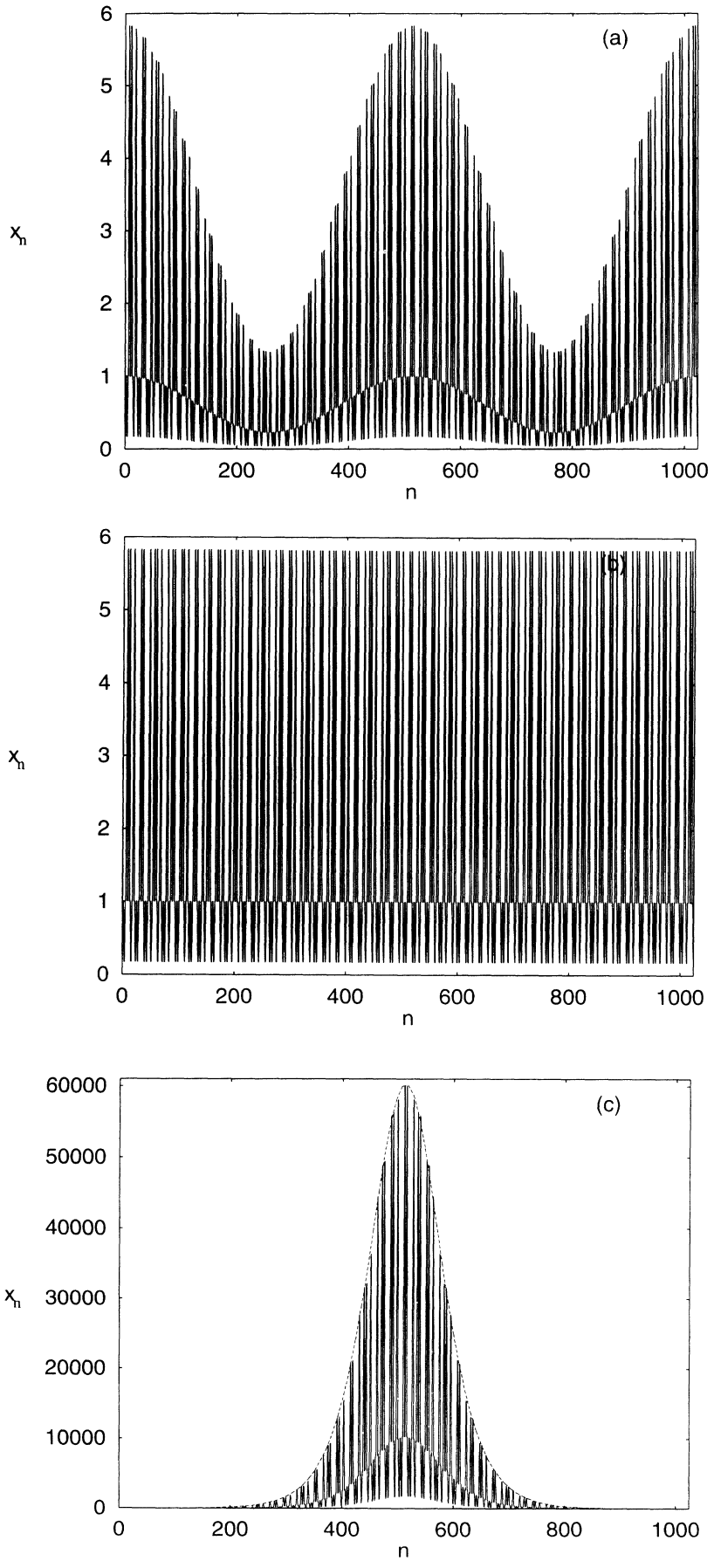

FIG. 5. Field intensities x_n versus position for the nonlinear Thue-Morse chain with $\alpha=-10^{-8}$ corresponding to different peaks in Fig. 4(b). (a) $E\approx 0.414\,277\,8$, (b) $E\approx 0.414\,228\,2$, (c) $E\approx 0.413\,980\,633$, (d) $E\approx 0.413\,559\,738\,3$, (e) $E\approx 0.413\,194\,797\,45$, and (f) $E\approx 0.411\,479\,875\,839\,722\,44$. In all cases, $N=1024$, $k=0.01$, $|T|^2=1$, and $t\approx 1$. The dashed line in (c) is a plot of the function $60300/\cosh^2[0.0116(n-513)]$. The peak corresponding to (f) is too narrow to be visible in Fig. 4(b).

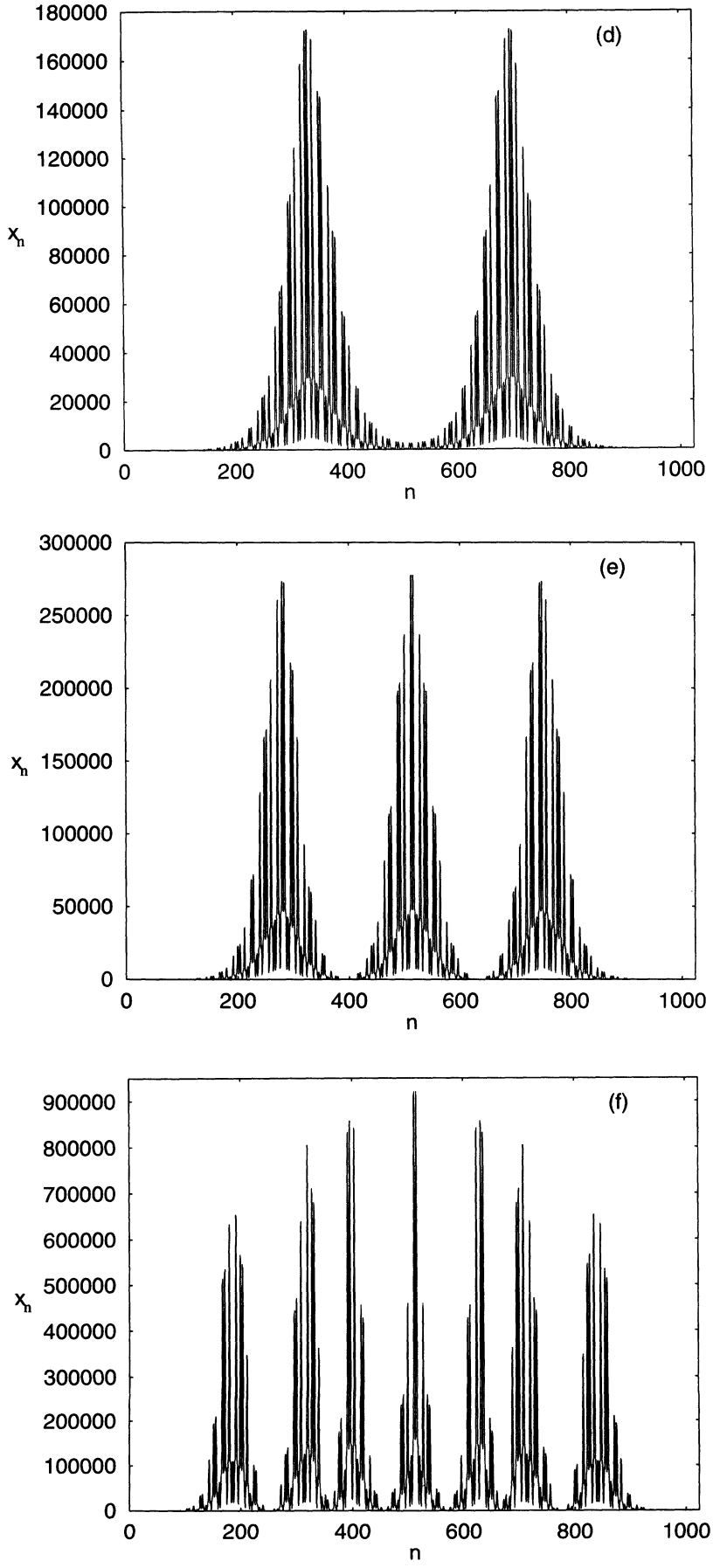

FIG. 5. (*Continued*).

we show the second modulated state in the linear transmitting region and the state closest to the linear gap edge, respectively. They are both very similar to the states giving rise to the corresponding transmission peaks in the linear case. Figure 5(c) shows the field intensity for the first peak yielding perfect transmission when entering the linear gap region from the band edge. As can be seen, the envelope is almost perfectly fitted by the square of Eq. (4), showing that it indeed is the existence of solitonlike structures as discussed in Sec. II that gives rise to this transmission peak.

When going further into the linear gap region, one finds new peaks giving perfect transmission. The field intensity for the second gap peak is shown in Fig. 5(d), showing that it can be viewed as a pair of two weakly interacting fundamental solitons of the type previously discussed. Excitation of this kind of higher-order soliton, a "multisoliton" or "soliton train," has been reported in different contexts for periodic systems.[16–18] Note that although the complete object looks symmetric with respect to the center of the chain, each of the two "soliton peaks" will be asymmetric due to the interaction between them. The third peak having $t=1$ in the gap in Fig. 4(b) corresponds, as expected, to a similar object consisting of three closely spaced solitons [Fig. 5(e)]. As the energy distance from the gap edge increases, the width of each fundamental soliton in the multisoliton will be smaller and its amplitude larger. Also, the width of each transmission peak in Fig. 4(b) will decrease, so that peaks resulting from multisolitons of higher order than 3 will not be resolved in this figure. However, such structures will occur until each solitonlike object will be so narrow that it is affected by the discrete nature of the lattice. [See Fig. 5(f) for the case with seven interacting fundamental solitons.]

As $|\alpha|$ is increased, the amplitude of each fundamental

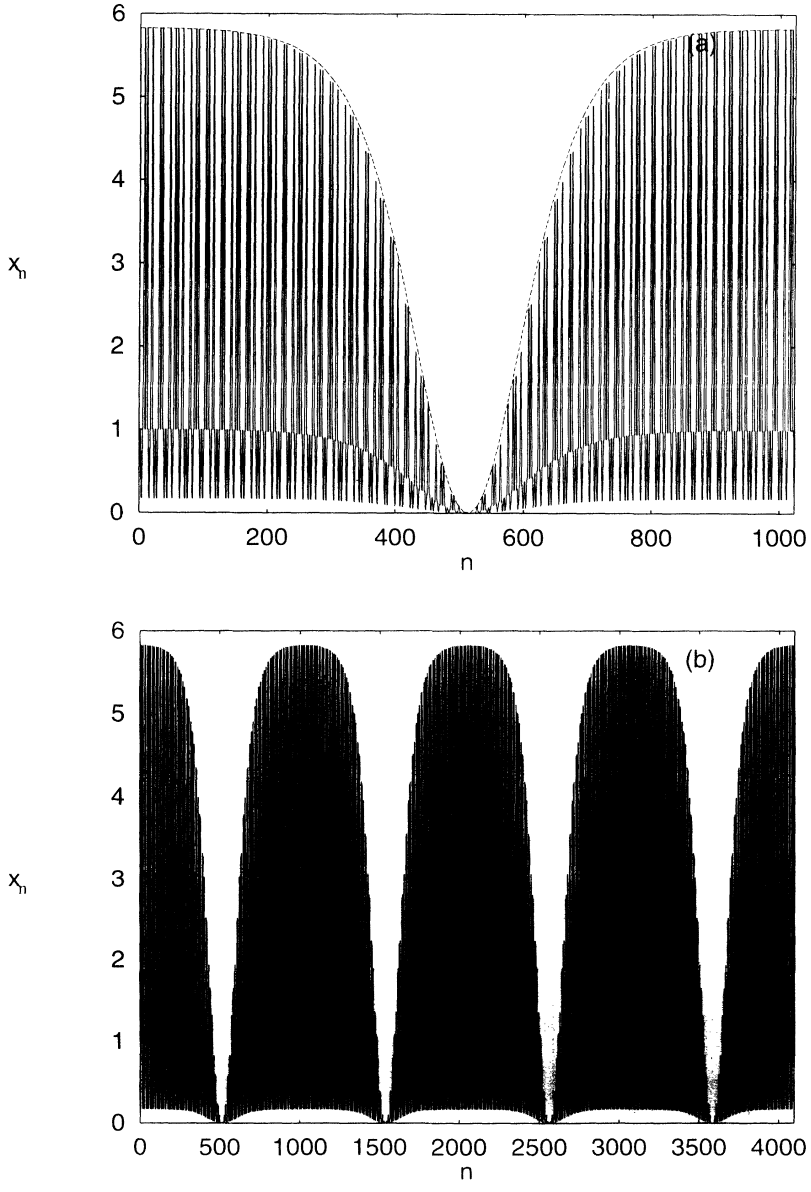

FIG. 6. (a) Same as in Fig. 5 but with $\alpha=5\times10^{-5}$ and $k=10^{-5}$ for the transmission peak closest to the gap region, having $E=0.414\,438\,933\,53\ldots$. The dashed line is a plot of the function $5.83\tanh^2[0.0084(n-513)]$. (b) Field intensity for the object giving perfect transmission for the energy closest to that in (a) ($E=0.414\,438\,933\,600\,477\ldots$) when $N=4096$.

soliton will decrease, and its width will increase. Also, more peaks yielding high but nonperfect transmission will develop in the linear gap region. This is shown in Fig. 4(c), which shows the transmission coefficient in the same region as Figs. 4(a) and 4(b) but with $\alpha=-10^{-4}$. The broad transmission resonance in the middle of the figure actually consists of two neighboring peaks, one corresponding to an edge state with uniform amplitude as in Fig. 5(b), and one corresponding to a multisoliton with four small-amplitude peaks. The single soliton and the multisoliton states having fewer than four peaks have for this value of the nonlinearity constant grown too wide and too flat to be separately distinguished, and are assimilated into the edge state. Similarly, the first three modulated band states have also disappeared, and the first peak to the right of the broad peak in Fig. 4(c) corresponds to the case when the chain length is four times the modulation wavelength. The case when $|\alpha|$ is of the same order of magnitude as the on-site energy and hopping integral will be discussed in Sec. IV.

When α takes a small positive value, there will be no transmission peaks in the linear gap region, and the peaks in the linear band region will be shifted an amount of the order of α in the positive energy direction. However, as was discussed in the introduction, for a positive nonlinearity constant it is for a periodic system at a lower band edge possible to have peaks with perfect transmission due to so-called dark solitons, described by Eq. (5) and appearing as a dip in a constant background intensity. For the Thue-Morse system in the energy region discussed above, we also find for certain parameter values transmission peaks that are due to the formation of such objects. This is shown in Fig. 6(a), where the intensity distribution corresponding to the transmission peak closest to the gap when $\alpha=5\times10^{-5}$ and $k=10^{-5}$ is fitted to the square of Eq. (5) with empirical values of C and γ. The value of k is here chosen to be smaller than in the previous examples, since a somewhat larger value of k will give the result that the intensity retains a nonzero minimum value. Since the background intensity for each of the three subsequences in the dark soliton is independent of α and E [the values are 1 and $(\sqrt{2}\pm1)^2$ just as for the linear system], the width of the soliton will be roughly proportional to $1/\sqrt{\alpha}$ as for periodic systems. The decrease of soliton width with increasing α (or, equivalently, increasing transmitted intensity) is in contrast to the previously discussed feature of the bright soliton, where the decrease of soliton amplitude causes its width to increase with increasing nonlinearity.

In a similar way as for the bright solitons, dark solitons may also combine to form multisolitons. Figure 6(b) shows the field intensity of the object giving perfect transmission at approximately the same energy as in Fig. 6(a) when the length of the nonlinear chain is increased to 4096 sites. As can be seen, it consists of four coupled dark solitons of the type discussed above.

IV. THE TRANSMISSION PROBLEM, LARGE NONLINEARITY

As we have seen in the previous section, the main effect of the nonlinearity on the Thue-Morse transmission spectrum for small $|\alpha|$ is, besides the change in energy scale which is of order α, the development of transmission peaks due to soliton resonances in the nontransmitting regions of the corresponding linear system. The linear transmitting regions will still be transmitting when a small nonlinearity is added. However, as the nonlinearity becomes larger in magnitude, transmitting and nontransmitting regions will be mixed in a more complex way. The description of this behavior is perhaps most easily visualized by plotting the "stability zone," which is the set of points in the (E,α) plane where the map (10) yields bounded orbits, or, equivalently, a nonzero transmission coefficient. For periodic systems with $V_n\equiv0$, this is a connected set with inversion symmetry possessing a fractal boundary.[29,30] The orbits belonging to this set are either periodic, quasiperiodic, or chaotic.[29,30]

For a deterministic aperiodic system, the stability zone will in general have an even more complex structure than in the periodic case, due to the highly fragmented nature of the band structure of the corresponding linear system. In the specific case of the Thue-Morse sequence, it has been shown[11] that the spectrum of allowed energies for the infinite linear system is a Cantor set of zero Lebesgue measure. In this context, this implies that if we pick an energy value at random, the corresponding orbit of Eq. (10) will with probability 1 eventually diverge. However, because of the Cantor-set nature of the spectrum, a study of a finite system will give us a picture of the spectrum of the infinite system, as if obtained with finite resolution. As it turns out, when the nonlinearity constant takes values of the same order as the hopping integral and on-site energy, the energy intervals giving bounded orbits quickly become very narrow when the length of the nonlinear chain increases. So, to give a picture of where in the (E,α) plane those orbits are located, we are for computational reasons restricted to studying rather short systems. In Fig. 7(a) we show a plot of the set of points giving nondiverging orbits for a nonlinear Thue-Morse chain of length $N=64$, obtained by a step procedure using step lengths of 10^{-4} in E and 2×10^{-5} in α. The value of k has been chosen in a similar way as in Ref. 30 to take the value $k=\arccos(-E/2)$ when $-2<E<2$, and to take a small value ($k=0.01$) if $E\le-2$, and a value close to π ($k=\pi-0.01$) if $E\ge2$. The separation of the unbounded orbits from the bounded ones is practically performed by using an upper cut-off at $x_n=10^{35}$. The result is not sensitive to the specific value of the cutoff, since an orbit once entering the unbounded regime will diverge very rapidly [roughly as $\exp(3^L)$].[29]

As can be seen, the stability zone for the Thue-Morse system plotted in Fig. 7(a) does not possess the inversion symmetry previously discussed for a periodic system with $V_n\equiv0$, even though the spectrum of the linear Thue-Morse model is symmetric around $E=0$. This symmetry breaking is a general property of nonlinear models with nonzero on-site potentials, periodic or aperiodic. The symmetry however seems to be recovered if, in addition to changing the signs of E and α and changing k to $\pi-k$, one also changes the sign of the on-site potential at each site, i.e., $V\rightarrow-V$. The region containing the bounded

orbits is seen to consist of a complicated structure of different curves corresponding to orbits with similar features. However, for each fixed α the set of energies giving bounded orbits still seems to have a Cantor structure, and consequently each of the curves of bounded orbits will split as the chain length is increased into several new such curves divided by regions of unbounded orbits. In Fig. 8(a) we show an example of how the field intensities vary with position for a chain of length $N=8192$ for a point belonging to one of the stable curves of Fig. 7(a), with $\alpha=-0.015$ and $E\approx 0.090\,092\,4$. In order for the orbit to remain stable over the whole chain, the energy had to be specified with 93 digits of accuracy. One can note that for these particular parameter values, the field intensities are grouped into a number of different "bands" which only occasionally mix with each other. In this aspect, it looks similar to the quasiperiodic orbits occurring for periodic systems with large nonlinearity.

If k is chosen in a different way than in Fig. 7(a), there will still be a similar mixture of regions in the (E,α) plane giving bounded and unbounded orbits, but the stability zone will in general look different for different values of k. In particular, we find that if k is chosen to a small value, stable orbits will exist even for rather large values of α. Figure 7(b) shows the plot corresponding to Fig. 7(a) when $k=0.01$ for all energies. It can be seen that even values of α with a modulus larger than 2.0 give bounded orbits for some energies. For these large nonlinearities, however, the energy intervals giving bounded orbits for a fixed chain length become extremely narrow. As an example, we show in Fig. 8(b) the field intensities obtained starting from the site $N=4096$ when $\alpha=1.5$ and $E\approx 0.133\,600\,28$. In this plot, we have specified the energy with 250 digits of accuracy, but in spite of this high accuracy the orbit will begin to diverge at approximately $n=1800$. (Of course, it would still be possible to obtain a

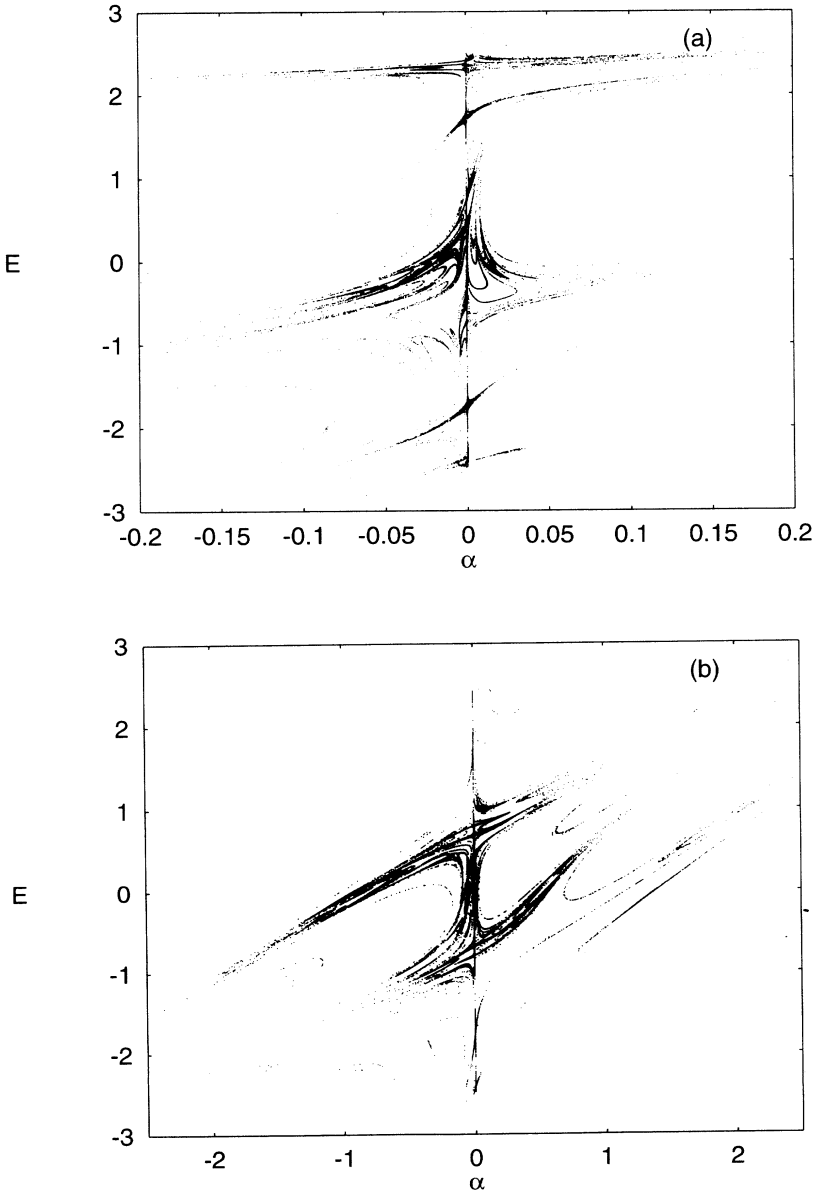

FIG. 7. (a) "Stability zone" showing the points in the (E,α) plane where the map (10) gives nondiverging orbits for a Thue-Morse system of length $N=64$. The resolution is 10^{-4} on the energy axis and 2×10^{-5} on the α axis. The value of k is chosen as $k=\arccos(-E/2)$ if $-2<E<2$, $k=0.01$ if $E\leq -2$, and $k=\pi-0.01$ if $E\geq 2$. (b) Same as in (a) but with $k=0.01$ independent of E. Here, the resolution is 5×10^{-4} in E and 5×10^{-5} in α.

bounded orbit for any chain length by specifying more decimals of E, but this would rapidly increase the computation time.) As can be seen, this orbit seems to have a chaotic structure, in contrast to the case previously discussed.

V. SUMMARY

We have studied properties of systems described by a tight-binding version of the nonlinear Schrödinger equation with a deterministic aperiodic on-site potential. One of the main purposes of this paper has been to show that solitonlike wave functions may occur in this type of nonlinear system even if they are aperiodically modulated. For this purpose, we have concentrated our studies on the on-site Thue-Morse model, where the existence of extended, Bloch-like eigenstates in the linear model indicates that it has properties close to those of a periodic system. By solving a nonlinear eigenvalue problem self-consistently, we find wave functions well described by the envelope soliton (4) for small values of the nonlinearity constant. This type of states is shown to result in peaks of perfect transmission in the linear transmission gap, when a problem involving stationary transmission of single Bloch waves through the nonlinear, aperiodic chain is studied. Dark solitons, described by Eq. (5) and appearing as a dip in the background intensity, are also found to yield peaks of perfect transmission. Two types of higher-order solitons, which can be viewed as combinations of weakly interacting fundamental solitons of the bright and dark type respectively, are shown to cause sequences of peaks in the transmission spectrum. For larger nonlinearities, i.e., for values of the nonlinearity constant of the same order as the hopping integral and on-site energy, we have studied the set of points in the

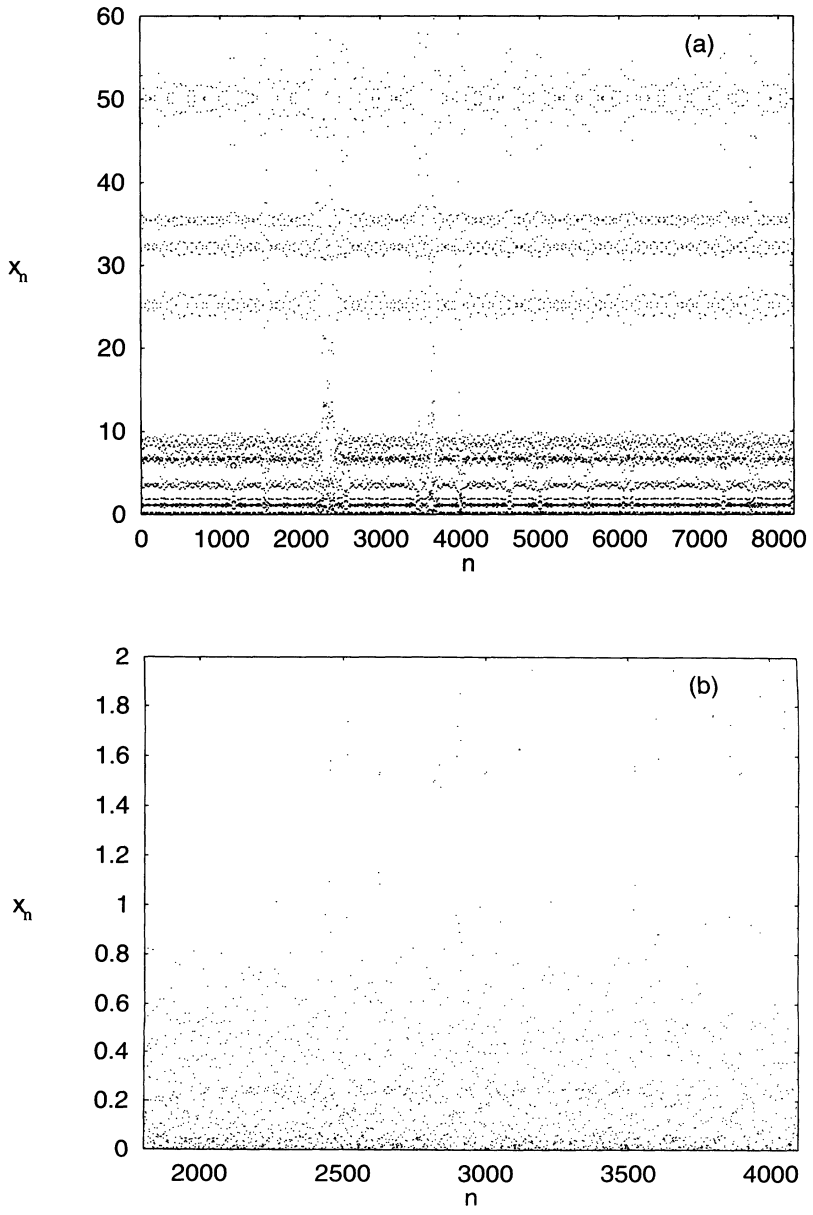

FIG. 8. (a) Field intensity versus position for a point belonging to the stability zone in Fig. 7(a), $\alpha=-0.015$, $E\approx 0.090\,092\,4$, and $k=\arccos(-E/2)$. The energy has been specified with 93 decimals in order for the orbit to stay bounded over 8192 sites. (b) Same as in (a) for a point from Fig. 7(b), $\alpha=1.5$, $E\approx 0.133\,600\,28$, and $k=0.01$; E being specified with 250 decimals. The orbit, starting at $N=4096$, will begin to diverge at $n\approx 1800$.

(E,α) plane where the map (13) describing the transmission problem gives bounded orbits (the stability zone) and discussed its Cantor-set structure.

When comparing our results for the Thue-Morse model with those of the Fibonacci model, we find that the critical nature of the eigenstates in the latter model will result in a nonlinear state being localized in a region of approximately the same size as for the corresponding Thue-Morse state, but having no smooth solitonlike envelope. In general, one might expect that solitonlike states may appear also in other aperiodic models possessing Bloch-like states,[31] while models possessing critical states will behave similarly to the Fibonacci case. The behavior of the Rudin-Shapiro system with its mainly localized states is also an interesting problem in this context, in view of the ongoing discussion on the interplay between disorder and nonlinearity. We have preliminary numerical results indicating that the exponentially localized states of the Rudin-Shapiro model will remain exponentially localized even in the presence of the nonlinearity, but we hope to be able to give a more detailed description of this in a future work.

ACKNOWLEDGMENTS

We would like to thank Mihnea Dulea for discussions about aperiodic systems. Access to the computer facilities at the National Supercomputer Center in Sweden at the University of Linköping has been very useful in performing parts of the numerical calculations in this work. Some of the numerical calculations in Sec. IV have been performed using the multiple-precision floating-point computation package MPFUN developed by David H. Bailey, NASA Ames Research Center. Financial support from the Swedish Natural Science Research Council is also gratefully acknowledged.

[1]A. Janner, T. Janssen, and P. M. de Wolff, Europhys. News **13**, 1 (1982), and references therein.

[2]D. Shechtman, I. Blech, D. Gratias, and J. W. Cahn, Phys. Rev. Lett. **53**, 1951 (1984).

[3]R. Merlin, K. Bajema, R. Clarke, F. Y. Juang, and P. K. Bhattacharya, Phys. Rev. Lett. **55**, 1768 (1985).

[4]S. Aubry and G. André, Ann. Israel Phys. Soc. **3**, 133 (1980); C. M. Soukoulis and E. N. Economou, Phys. Rev. Lett. **48**, 1043 (1982); J. Avron and B. Simon, Duke Math. J. **50**, 369 (1983); H. Hiramoto and M. Kohmoto, Phys. Rev. Lett. **62**, 2714 (1989); H. Hiramoto and M. Kohmoto, Phys. Rev. B **40**, 8225 (1989); J. F. Weisz, M. Johansson, and R. Riklund, *ibid.* **41**, 6032 (1990); M. Johansson and R. Riklund, *ibid.* **42**, 8244 (1990).

[5]A. Thue, Norske vid. Selsk. Skr. I. Mat. Nat. Kl. Christiania **7**, 1 (1906); M. Morse, Trans. Am. Math. Soc. **22**, 84 (1921).

[6]H. S. Shapiro, M.S. thesis, Massachusetts Institute of Technology, 1951; W. Rudin, Proc. Am. Math. Soc. **10**, 855 (1959).

[7]M. Kohmoto, L. P. Kadanoff, and C. Tang, Phys. Rev. Lett. **50**, 1870 (1983); S. Ostlund, R. Pandit, D. Rand, H. J. Schellnhuber, and E. G. Siggia, *ibid.* **50**, 1873 (1983).

[8]A. Sütö, J. Stat. Phys. **56**, 525 (1989); J. Bellissard, B. Iochum, E. Scoppola, and D. Testard, Commun. Math. Phys. **125**, 527 (1989).

[9]M. Kohmoto, B. Sutherland, and C. Tang, Phys. Rev. B **35**, 1020 (1987); M. Kohmoto, Int. J. Mod. Phys. B **1**, 31 (1987).

[10]R. Riklund, M. Severin, and Y. Liu, Int. J. Mod. Phys. B **1**, 121 (1987); F. Axel and J. Peyrière, J. Stat. Phys. **57**, 1013 (1989); J. Bellissard, in *Number Theory and Physics,* edited by J. M. Luck, P. Moussa, and M. Waldschmidt, Springer Proceedings in Physics, Vol. 47 (Springer-Verlag, Berlin, 1990), p. 140; C. S. Ryu, G. Y. Oh, and M. H. Lee, Phys. Rev. **46**, 5162 (1992).

[11]J. Bellissard, A. Bovier, and J.-M. Ghez, Commun. Math. Phys. **135**, 379 (1991).

[12]M. Dulea, M. Johansson, and R. Riklund, Phys. Rev. B **45**, 105 (1992).

[13]M. Dulea, M. Johansson, and R. Riklund, Phys. Rev. B **47**, 8547 (1993).

[14]A. Bovier and J.-M. Ghez, Commun. Math. Phys. **158**, 45 (1993).

[15]H. Hiramoto, J. Phys. Soc. Jpn. **59**, 811 (1990); H. Hiramoto and M. Kohmoto, Int. J. Mod. Phys. B **6**, 281 (1992).

[16]T. Holstein, Ann. Phys. (N.Y.) **8**, 325 (1959); L. A. Turkevich and T. D. Holstein, Phys. Rev. B **35**, 7474 (1987).

[17]L. Kahn, N. S. Almeida, and D. L. Mills, Phys. Rev. B **37**, 8072 (1988).

[18]G. P. Agrawal, in *Contemporary Nonlinear Optics,* edited by G. P. Agrawal and R. W. Boyd (Academic, Boston, 1992), and references therein.

[19]S. A. Gredeskul and Yu. S. Kivshar, Phys. Rep. **216**, 1 (1992), and references therein.

[20]P. W. Anderson, Phys. Rev. **109**, 1492 (1958).

[21]B. Doucot and R. Rammal, Europhys. Lett. **3**, 969 (1987).

[22]J. Fröhlich, T. Spencer, and C. E. Wayne, J. Stat. Phys. **42**, 247 (1986); C. Albanese and J. Fröhlich, Commun. Math. Phys. **116**, 475 (1988); C. Albanese, J. Fröhlich, and T. Spencer, *ibid.* **119**, 677 (1988); M. J. McKenna, R. L. Stanley, and J. D. Maynard, Phys. Rev. Lett. **69**, 1807 (1992).

[23]P. Devillard and B. Souillard, J. Stat. Phys. **43**, 423 (1986); Q. Li, C. M. Soukoulis, St. Pnevmatikos, and E. N. Economou, Phys. Rev. B **38**, 11 888 (1988); R. Bourbonnais and R. Maynard, Phys. Rev. Lett. **64**, 1397 (1990); Yu. S. Kivshar, S. A. Gredeskul, A. Sánchez, and L. Vázquez, *ibid.* **64**, 1693 (1990); D. L. Shepelyansky, *ibid.* **70**, 1787 (1993).

[24]S. Dutta Gupta and D. S. Ray, Phys. Rev. B **38**, 3628 (1988); *ibid.* **40**, 10 604 (1989); *ibid.* **41**, 8047 (1990).

[25]L. M. Kahn, K. Huang, and D. L. Mills, Phys. Rev. B **39**, 12 449 (1989).

[26]M. Kohmoto, B. Sutherland, and K. Iguchi, Phys. Rev. Lett. **58**, 2436 (1987).

[27]St. Pnevmatikos, O. Yanovitskii, Th. Fraggis, and E. N. Economou, Phys. Rev. Lett. **68**, 2370 (1992).

[28]K. Schmidt and M. Springborg, Synth. Met. **55-57**, 4473 (1993); J. Phys. Condens. Matter **5**, 6925 (1993).

[29]F. Delyon, Y.-E. Lévy, and B. Souillard, Phys. Rev. Lett. **57**, 2010 (1986).

[30]Y. Wan and C. M. Soukoulis, Phys. Rev. B **40**, 12 264 (1989); Phys. Rev. A **41**, 800 (1990).

[31]M. Severin, M. Dulea, and R. Riklund, J. Phys. Condens. Matter **1**, 8851 (1989).

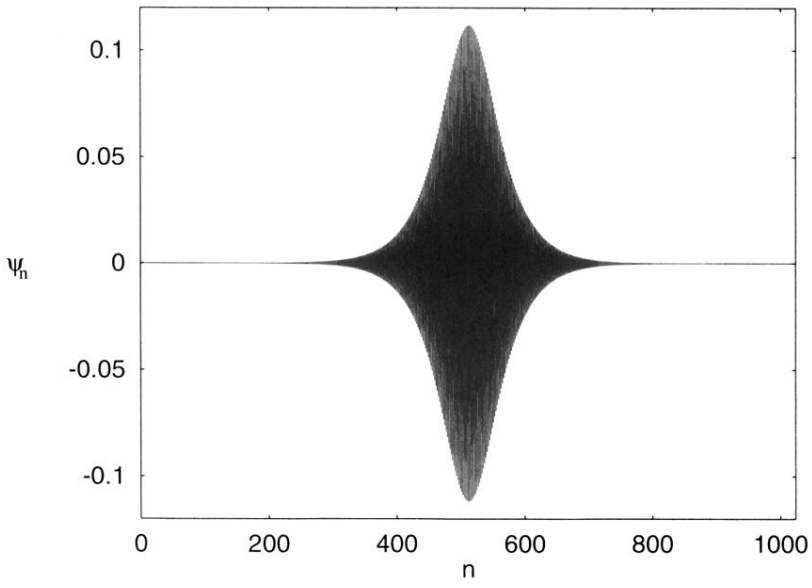

FIG. 1. Normalized wave function corresponding to the highest energy obtained as a self-consistent solution to (2) when $V_n \equiv 0$, $\alpha = 0.1$, and $N = 1024$. The energy E is given by $E = 2.000\,625\,076\ldots \approx 2+\gamma^2 = 2+\alpha^2/16$.

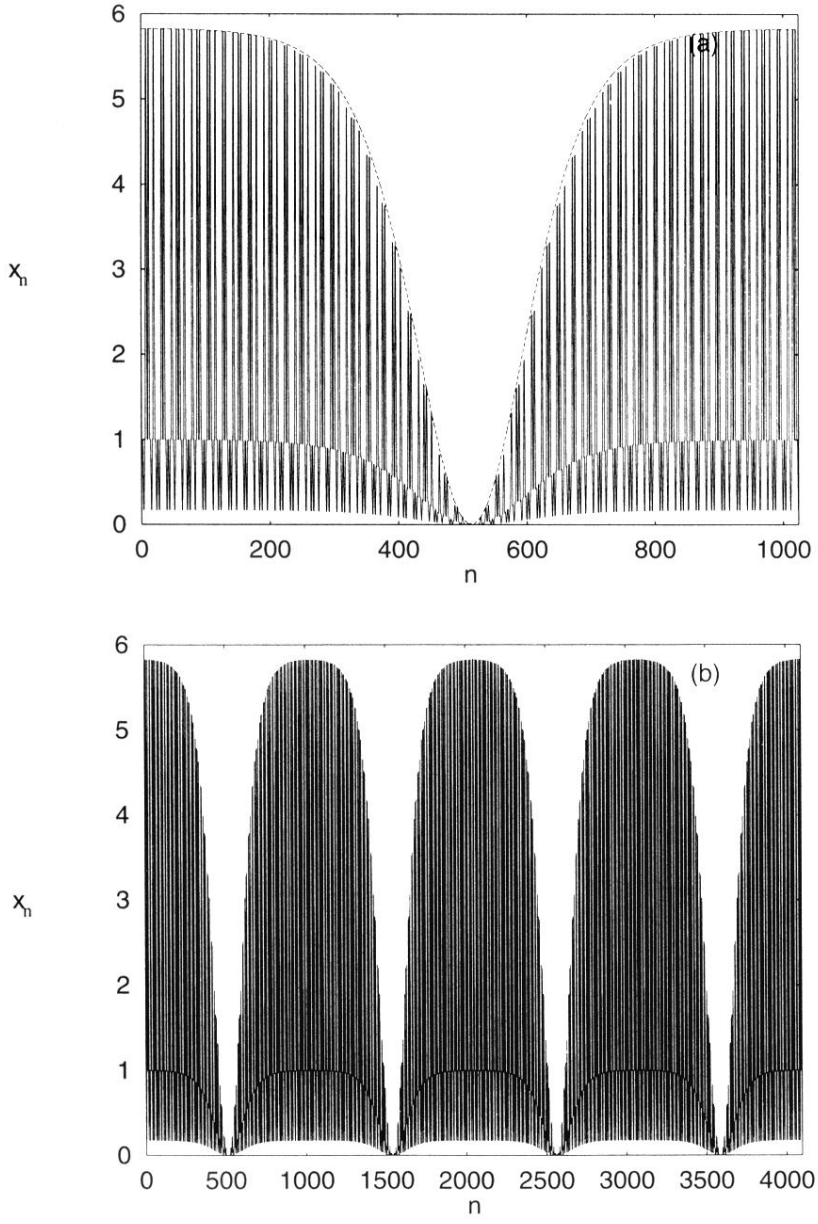

FIG. 6. (a) Same as in Fig. 5 but with $\alpha=5\times10^{-5}$ and $k=10^{-5}$ for the transmission peak closest to the gap region, having $E=0.414\,438\,933\,53\ldots$. The dashed line is a plot of the function $5.83\tanh^2[0.0084(n-513)]$. (b) Field intensity for the object giving perfect transmission for the energy closest to that in (a) ($E=0.414\,438\,933\,600\,477\ldots$) when $N=4096$.